RESEARCH ON SRV ESTIMATION ALGORITHM BASED ON TRIANGULAR MESH SUBDIVISION

XULIN WANG[1],MENGQIONG YANG[2]

[1]*College Of Marine Geosciences,Ocean University Of China,Qingdao 266100,P.R.China. wangxulin@stu.ouc.edu.cn*
[2]*Hubei Liantou Mining Co., LTD,Hubei United Investment,WuHan 430061, P.R.China.1285604123@qq.com*

(Received February 8, 2022; revised version accepted December 20, 2022)

ABSTRACT

Fracturing has emerged as a powerful technique to improve well production and the recovery of unconventional reservoirs. Under this background, the present research aims to improve the accuracy of SRV estimation. Currently speaking, a common method used to estimate SRV is by constructing a mathematical model. However, there are certain drawbacks associated with this method, like rough fitting effect and low estimation accuracy. In response to this problem, we propose a new SRV estimation method based on a combination of computer three-dimensional modeling methods and the triangular mesh subdivision method to subdivide the three-dimensional envelope structure formed by the microseismic point cloud as well as the volume of the ineffective fracturing area inside the fracturing reformation area. The rejection improves the calculation accuracy of SRV without changing the original distribution characteristics of the microseismic point cloud. Moreover, the final reservoir fracturing model is more accurate The proposed method is validated by a collection of measured data and the corresponding results prove the effectiveness of this method.

KEY WORDS: Stimulated reservoir volume, Delaunay triangulation, Minimum volume ellipsoid, Mesh subdivision

0963-0651/23/$5.00

INTRODUCTION

As one of the emerging clean energy sources in the world, shale gas resource has attracted tremendous international attention and has promising development prospects. As a low-permeability oil and gas reservoir, shale reservoir has physical characteristics such as low porosity, low permeability and low connectivity. and thus need to be modified by fracturing to improve their petrophysical properties, but thankfully shale reservoirs are highly brittle and have a considerable number of natural gas-rich fractures, and. If such natural fractures can be broken and transported through horizontal wells, shale gas production will certainly witness a sharp increase (Ren et al. 2018; Peng et al. 2019). The complex fracture network area formed by broken natural fractures is called “Reservoir Reconstruction Volume” (SRV). The real data analysis suggests that SRV demonstrates a strong positive correlation with shale gas production. Accordingly, the accurate estimation of shale gas reservoir is of great importance for the evaluation of fracture design effectiveness as well as production capacity prediction (Sakhaee et al. 2012; Walton et al. 2013).

Currently, SRV estimation has been measured by either precision equipments or mathematical model fitting (Shao et al. 2017). Precision equipments like microseismic monitors estimate SRV with the location of microseismic signals by monitoring seismic signals in real time. Theoretically speaking, the more accurate the measured microseismic signal data is, the more reliable the SRV estimation results are. However, the detection is costly and large-scale application is deemed impractical. Another popular precision equipment, the electronic inclinometer, estimates SRV by measuring the small dip angle of the fractured reservoir surface, which is less costly and simple to operate experimentally. The major problems with this method are low calculation accuracy and imprecise SRV estimation (Hu et al. 2014; Seale et al. 2006; King et al. 2010; Cipolla et al. 2010). As a result, mostscholars choose to construct a 3D model to estimate SRV with mathematical methods. For example, SRV can be estimated by seam network length, width and height (Fisher et al. Warpinski; Warpinski et al. 2008, 2009). In the same vein, the width of SRV is measured by fracture half-length and fracture spacing, and the length of SRV is measured by horizontal well length (Mayerhofer et al. 2010). Some scholars have analyzed the fracture network structure of fractured shale reservoirs and concluded that the fracture region caused by fracture modification appears a symmetric ellipse, thereby proposed a minimum closed ellipse model to approximate the size of SRV (Yu G. 2012; Xie et al. 2015; Wen et al. 2014) Previous studies have also proposed lineament network models and unconventional fracture extension models to simulate complex fracture patterns (Xu et al. 2009; Weng et al. 2011). However, rule-based mathematical geometric models such as cubic and ellipsoidal approaches to estimate SRV ignore the complexity of the microseismic event point distribution, and the constructed rule-based models include a large portion of the non- fractured area, which makes the final estimated SRV results large.

Based on the wireline network model and unconventional fracture extension model while the wireline network model is based on the simulation of complex fracture morphology, therefore, it requires high numerical accuracy in terms of input and cannot directly estimate SRV, which leads to a longer computational cycle. Therefore, how to improve the estimation method of SRV and the calculation accuracy of SRV in shale fracturing process is still an important issue.

With the advancement of 3D model construction methods in computer science, some scholars start adopting the irregular envelope method to estimate SRV, which has improved the accuracy of SRV estimation significantly compared with the above-mentioned regular model methods. The basis of this method is triangulation algorithm where the microseismic event points are first triangulated by spatial distance to form an overall convex polyhedron composed of several tetrahedral structures and the SRV is estimated by calculating the sum of volumes of all tetrahedral. The most pervasive triangulation algorithm at present is the Delaunay triangulation algorithm or a series of improved algorithms based on the Delaunay triangulation algorithm (Liu et al. 2019; Shao et al. 2018).Nevertheless, the SRV results obtained on the basis of triangulation algorithm still have problems in terms of accuracy. This is partly because triangulation algorithm cannot effectively perform calculations on non-convex data sets. Besides, when there are non-breaking regions in the microseismic event point distribution, the triangulation algorithm will take these invalid regions into account.

The accuracy of SRV estimation is of great significance to the exploration and development of shale gas reservoirs. Improving the accuracy of SRV estimation can not only effectively evaluate the shale gas production effect after fracturing, but also provide effective guidance for pre-fracturing construction design. To address the problem that the current SRV estimation algorithm cannot calculate the SRV of complex microseismic events well, this paper proposes a grid subdivision-based SRV estimation algorithm, which first eliminates the anomalous localization points by the DBSCAN algorithm, and then uses the grid subdivision algorithm to eliminate the internal invalid regions on the basis of the initial envelope formed by the triangular dissection algorithm, thus improving the accuracy of SRV estimation. . Through a set of experimental data tests, the grid segmentation-based SRV estimation algorithm proposed in this paper is compared with the traditional SRV algorithm and the Delaunay triangulation algorithm. The results not only demonstrate the effectiveness of this new method, but also show that it can provide an optimal design solution for fracture modification of shale gas reservoirs.

The Principle of SRV calculation method

DBSCAN clustering algorithm

In the process of shale fracturing, the microseismic monitoring results are affected by various factors such as errors in the velocity construction model. As a consequence, the first-arrival information of microseismic events cannot be collected accurately. Therefore, it is necessary to pre-process the microseismic event points prior to SRV calculation in order to eliminate some effects of the above factors. The method adopted in this research is the DBSCAN density clustering algorithm. The DBSCAN algorithm can be roughly described as starting from a core point, continuously reaching the density of the surrounding area through certain principles and finally forming a boundary region based on the core point where any two data points are density reachable (Shou et al. 2019; Sheridan et al. 2020; Wang et al. 2021; Chen Y et al. 2018; Alzaalan et al. 2012).The basic concepts of the DBSCAN algorithm are shown below:

Neighborhood: For any given data point a , its ε neighborhood is defined as:

$$N_{\varepsilon}(a) = \{q \in D \; dist(a, q) \leq \varepsilon \} \tag{1}$$

Density: Let $x \in X$, the expression of density: $\rho(x) = N_{\varepsilon}(x)$.

Core point: If $\rho(x) \geq MinPts$, x is the core point in X , the set around which the core point formed is X .

Boundary points: $x \in X_C / X$, x exists within the neighborhood of a core point, but a boundary point can exist in the neighborhood of multiple core points.

Noise point: A data point that is neither a core point nor a boundary point.

Eps and MinPts are the most critical parameters of the whole algorithm which refer to the maximum distance between sample points in a single cluster (also called the cluster radius) and the minimum number of sample points contained in a single cluster, respectively. If the number of sample points within the Eps neighborhood of a sample point is not less than the size of MinPts, then the sample point can be defined as the core point. If Eps is longer than the shortest distance from the sample point to its core point, it implies that it is direct density reachable from the sample point to the core point. For a sample point sequence, the sample points should meet the direct density reachable in turn. In other words, the direct density reachable should meet the transferability so that these sample points are density reachable. If two sample points are density reachable for the same point, then the two sample points are density connected.

Introduction of triangular mesh subdivision algorithm

3D surface reconstruction has great applicability in the field of computer vision reconstruction and mesh subdivision is one of the most popular methods.

By subdividing the target data set into surfaces several times, the shape of data points can be presented more accurately. The built model is smooth and flat with much-improved visuality and accuracy (Hu and Zhang 2016). The most typical triangular mesh subdivision algorithm is the LOOP subdivision method which is a subdivision method proposed by American scholar Charles Loop in his master's thesis in 1987 for approximate triangular surface segmentation (Biermann H et al. 2000; Devillers et al. 2011; Kim et al. 2019). This method focuses on subdividing a triangular surface by dividing an original triangular surface slice into four new triangular surface slices. The segmentation process can be roughly divided into two steps: the first step calculates the boundary points, and the second step moves the original vertices to generate a smooth surface with continuous tangents accordingly.

Calculating the boundary points

Calculating all the triangular facepieces to derive all the boundary points and non-boundary points. The model shown in Fig. 1 consists of two triangles up and down. The vertices of these two triangles are denoted by v_2 and v_3 , and the endpoints of the edges in vertices coordinates are denoted by v_0 and v_1 , respectively. If the two endpoints of an edge inside the mesh are v_0 and v_1 , and the faces of the two triangles sharing this edge are ($v0$, $v1$, $v2$) and ($v0$, $v1$, $v3$) , then the newly generated edge points are:

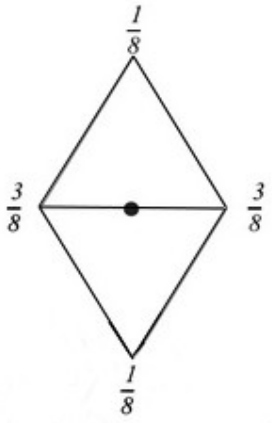

(2)

Fig. 1 Internal vertices

The difference between a mesh boundary E -vertex and a mesh interior E -vertex is that this edge lies at the boundary of the model and belongs to only one triangle; no second triangle shares this edge. Let

the two endpoints of this edge be v_O and v_1 , and the location of the newly

added vertex v Expression is:

A mesh boundary E -vertex and a mesh interior E -vertex differ in that this edge is located at the boundary of the model and only belongs to a triangle, without another triangle sharing this edge. Let the two endpoints of this edge be v_O and v_1 ,and the position of the newly added vertex v is denoted as:

(3)

Fig. 2 Generating boundary vertices

Updating the original points

The boundary needs to be processed so as to make the generated boundary smoother. Supposing the original interior vertice is $v0$, and the adjacent vertices are $v1$, $v2$, $v3$, and $v4$, then the coordinates of the shifted vertices v_0 are:

$$v = (1-n\beta)v_0 + \beta \sum v_i \tag{4}$$

Where v_i is the surrounding points of the original point v_0 , and the point n denotes the total number of surrounding points of the original point. The essence of the boundary shift is the weighted sum of the vertex itself and its neighboring vertices. The weight of the vertex itself is $1-n\beta$, and the weight of its neighboring points is β . Here the weight β is obtained by the following equation:

$$\beta = \frac{1}{n}\left[\frac{5}{8} - (\frac{3}{8} + \frac{1}{4}\cos\frac{2\pi}{n})^2\right] \tag{5}$$

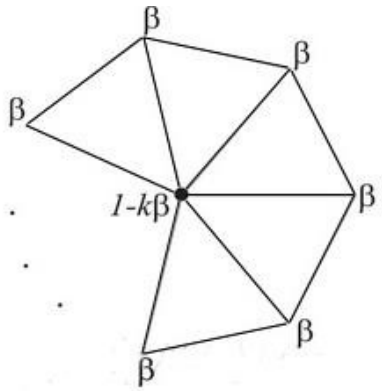

Fig. 3 Moving the original vertices (V-vertex)

If the boundary vertex v_0 has already existed and the two adjacent points of the vertex are v_1 and v_2, then the updated vertex position is:

$$v = \frac{3}{4}v_0 + \frac{1}{8}v_1 + \frac{1}{8}v_2 \tag{6}$$

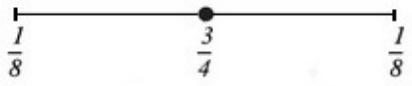

Fig. 4 Moving mesh boundary V-vertex

By performing a triangular dissection operation on a given set of microseismic event data points, one can obtain the index values of all triangular facet element vertexes. A mesh subdivision method is then applied in these triangular facet elements and the number of triangular facet elements are increased accordingly. For triangular side lengths which exceed normal range significantly, the distance between data points is shortened by differencing to form a tetrahedral combination structure composed of smaller triangles, and the overall fracture transformation volume size can be estimated by calculating all tetrahedral volumes within this structure. The formula for calculating the volume of tetrahedral is as

follows:

$$V = \begin{vmatrix} x_1 & y_1 & z_1 & 1 \\ x_2 & y_2 & z_2 & 1 \\ x_3 & y_3 & z_3 & 1 \\ x_4 & y_4 & z_4 & 1 \end{vmatrix} \times \frac{1}{6} \tag{7}$$

Where (x_1, y_1, z_1), (x_2, y_2, z_2), (x_3, y_3, z_3), (x_4, y_4, z_4) are the coordinate values of the four vertices in tetrahedron A, B, C , and D, respectively.

To illustrate the practical applicability of the mesh subdivision method, a set of data points with a total number of 200 are given in three-dimensional three plane to form a sphere. An initial sphere model is constructed using the Delaunay triangulation algorithm as shown in Figure 5 Then the model is subdivided by the mesh subdivision method and the number of subdivision set as two. Figure 6 and Figure 7 show the results for one and two subdivisions, respectively. Compared with the initial sphere structure in Figure 5 , the surface of the model obtained by the mesh subdivision method is smoother and more approximate to a spherical surface. Therefore, it is assumed that if the data points reach a considerable number, the model built with the mesh subdivision method can be more detailed.

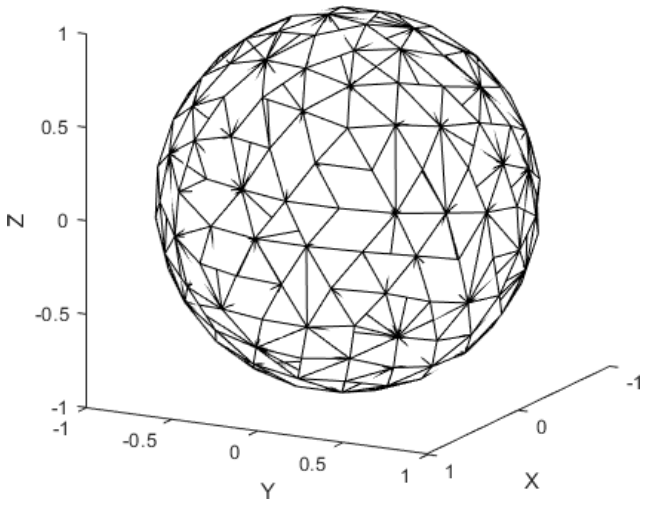

Fig. 5 Sphere model

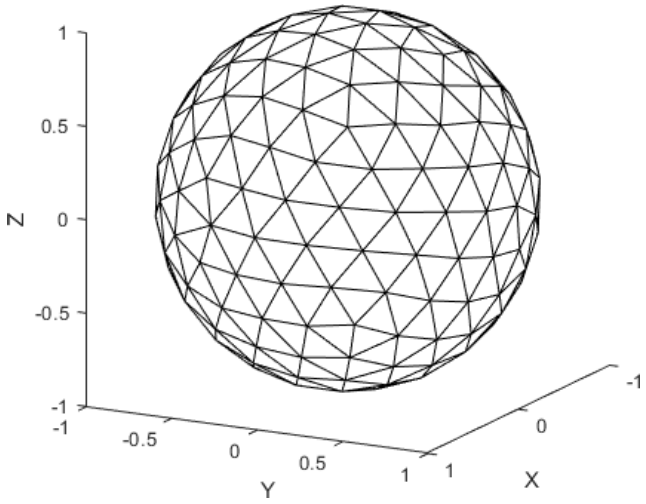

Fig. 6 Results of primary mesh subdivision

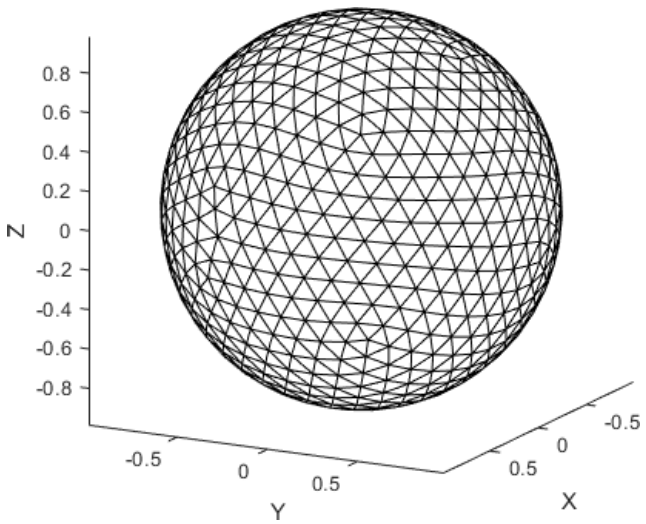

Fig. 7 Secondary mesh subdivision results

Introduction to the minimum volume ellipsoid algorithm

The rationale of the minimum volume ellipsoid algorithm is to fit microseismic event points by identifying the smallest ellipsoid in space. It is obtainable for the axis radius, ellipsoid center, and ellipsoid volume of the ellipsoid in the minimum ellipsoid building (Jie et al. 2018; Tao et al. 2017; Li et al. 2018; Halder 2018).

The minimum volume ellipsoid algorithm can be illustrated by the following equation:

$$E(a, A) = \{x \in R^3 \ (x - a)^T A(x - a) \leq 1\} \tag{8}$$

Where

$a \in R^3$

is the center point of the ellipsoid; $A \in R^{3\times3}$ is the symmetric positive definite matrix

$(\lambda_1, \lambda_2, \lambda_3)$ that controls the series of affine transformations of the ellipsoid and the inverse square root of the matrix eigenvalues is the length of the ellipsoid semi-axis that controls the scaling effect of the ellipsoid affine transformations. Meanwhile, the eigenvectors control the rotation effect of the ellipsoid affine transformations. Thus, the above equation can also be expressed as:

$$E = M_{translation} \times M_{rotation} \times M_{scaling} \times C \tag{9}$$

Where $M_{translation}, M_{rotation}, M_{scaling}$ denote the translational, rotational and stretching effects in the ellipsoidal affine variation, respectively; C is the unit sphere; E is the ellipsoid.

Solving the minimum volume ellipsoid problem can be converted to solving the optimization problem as follows:

$$\min_A \left[-(\Delta A)^{1/2}\right] \cdots \quad (x-a)^T A(x-a) \leq 1 \tag{10}$$

Using the KY algorithm (Kumar and Yildirim 2008), a convex optimization of the above equation can be performed so that the non-convex problem is changed to a convex problem for the optimal solution to obtain the centroid and volume size of the minimum volume ellipsoid.

Introduction of the Delaunay triangulation algorithm

The 3D Delaunay triangulation algorithm connects the discrete microseismic event points by triangulating the surface elements so as to form a tetrahedron to achieve the effect of faceting and bulking. The 3D Delaunay triangulation algorithm first establishes an initial tetrahedron as the initial envelope, and then processes the microseismic event points according to their various distances.

For example, for an event point, if the point is within the initial envelope, then the point shall be skipped and keep searching the next event point. If the point is not within the initial envelope, then a new triangular surface is randomly constructed by the point with points on the initial envelope,. If the triangular surface divides the point from the initial envelope, the initial envelope shall be expanded to form a new tetrahedral structure with the triangular surface as a face of the new tetrahedron (Xie et al. 2015; Zhou et al. 2013; Miao et al. 2019):

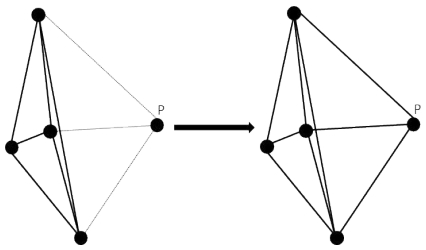

Fig. 8 Delaunay triangulation algorithm operation process

Example analysis

Solving SRV based on mesh subdivision method

The data used in this research are mainly from the local fracturing microseismic monitoring results of a shale well in a Chinese shale gas field. Due to the need of large-scale shale gas development, the shale gas reservoir was fractured in multiple sections in a horizontal well. The number of microseismic events is 70 and the corresponding spatial spreading extends in the east-west direction with the orientation close to vertical to the horizontal well. Figure 9 shows the microseismic monitoring results of the fractured section where the 3D XYZ axes show the spatial spreading size of the fractured area rather than the actual depth unit. Combined with the spatial spreading characteristics of microseismic events, a more concentrated cluster was formed after clustering by the DBSCAN algorithm with two parameters, Eps and MinPts, set to 40 and 2, respectively. Red dots in Figure 5 indicate the isolated anomalous localization points and black dots represent the formed clusters based on density.

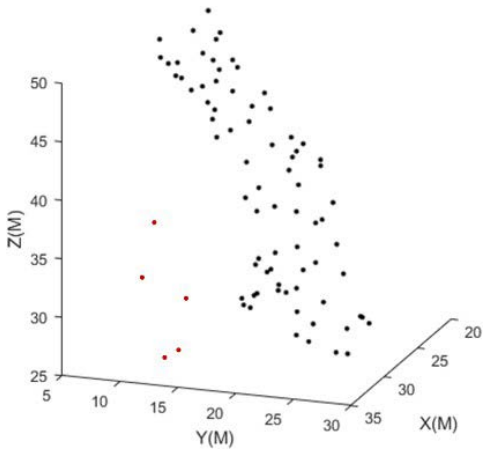

Fig. 9 Microseismic data monitoring results

After preprocessing the microseismic event points, the Delaunay triangulation method was used to calculate the microseismic event points, and the results of the initial 3D convex package consisting of multiple tetrahedra were obtained as can be seen from Figure 10 . Although the formed 3D convex package results include all microseismic event points, some non-fractured areas are also included, resulting in large SRV results for the final estimation, which cannot provide a better analysis of the fracture modification effect.

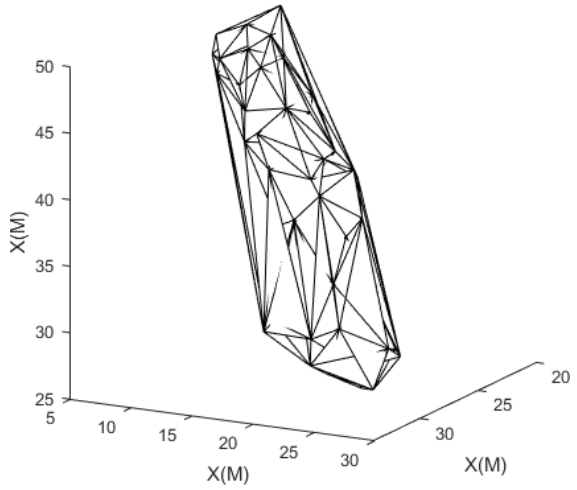

Fig. 10 Delaunay triangulation algorithm results

In order to exclude the non-fracture transformation area from the 3D convex package, all the surface index values and point coordinates of the 3D convex package are brought into the mesh subdivision algorithm, and a suitable number of subdivision iterations is set for excluding the non-fracture transformation area. Figure 11 and Figure 12 present the model results of subdivision once and twice, respectively. The model results obtained by subdividing twice are selected as the final reservoir fracturing transformation range. What stands out in Figure 12 is the difference compared with the results of the Delaunay triangulation algorithm operation in Figure 9 . The non-fracture transformation area in the reservoir is well eliminated and the model results generated are consistent with the distribution state of microseismic event points.

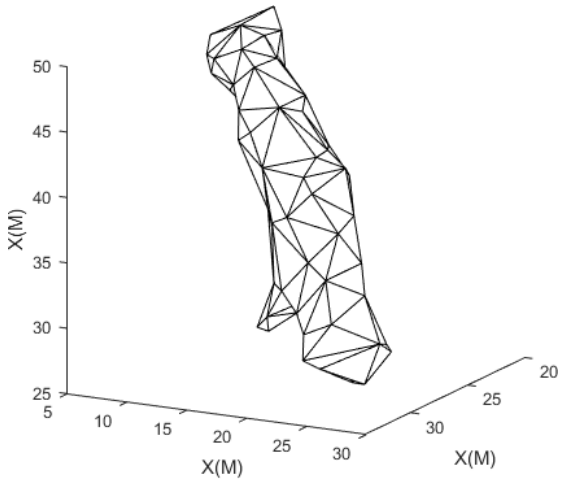

Fig. 11 Mesh subdivision processing results

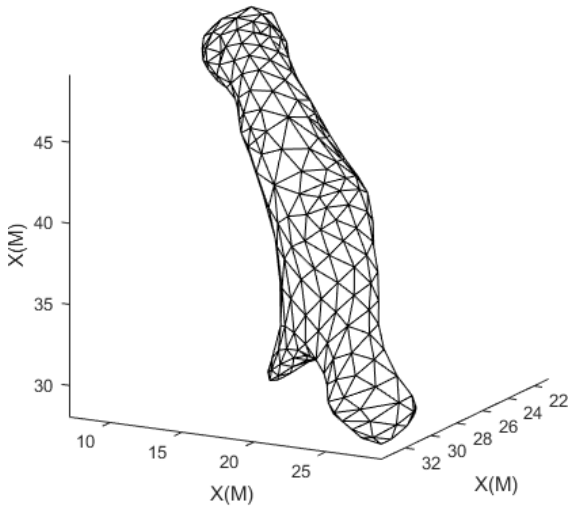

Fig. 12 Second-iteration subdivision processing results

Traditional method for solving SRV

In order to demonstrate the effectiveness of the mesh subdivision-based SRV estimation method proposed in this paper, the results are in comparison with those of the conventional orthocube method and the minimum volume ellipsoid algorithm, respectively. Figure 10 presents the model results generated by the Delaunay triangulation algorithm. Closer inspection of the figure shows that the model conforms with the spatial distribution of microseismic event points, but fractured regions are also included as shown in the red boxed area in Figure 13 below, which is due to the fact that the Delaunay triangulation algorithm cannot handle the error results caused by non-convex regions.

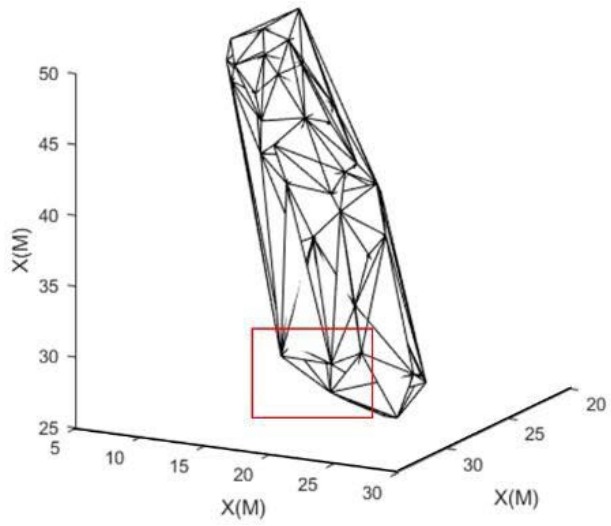

Fig. 13 Error region of Delaunay triangulation algorithm results

By calculating the microseismic data points with the minimum volume ellipsoid algorithm, one can obtain a minimum ellipsoid model with all microseismic data points as shown in 13 as well as the centroids and positive definite matrices of this model. The SRV size is then deduced by substituting

these parameters into Equation 10. An analysis of this ellipsoidal model reveals that the model structure is generally consistent with the distribution pattern of microseismic event points, but still covers a part of non-fracturing effective area. This is because the ellipsoid model itself is limited by a centrosymmetric geometry structure. As a result, model building is difficult when it comes to fitting the microseismic event points with uneven distribution or complex distribution pattern. It is fair to say that the traditional minimum volume ellipsoid algorithm is unsatisfied for model construction in terms of solving complex microseismic event points.

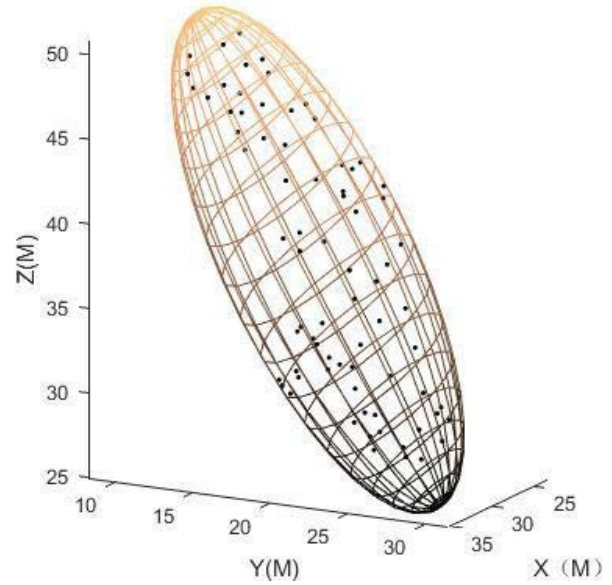

Fig. 14 Minimum volume ellipsoid algorithm model construction

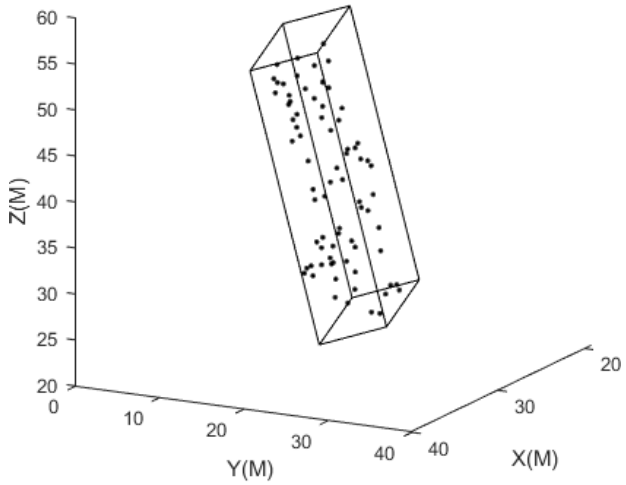

Fig. 15 Regular cube model construction

Figure 15 shows the model results of SRV estimation with the conventional cube method and the SRV can be obtained by calculating the volume of the cube. Based on a closer observation of the cube model it is apparent that the model is calculated with significantly low accuracy, with larger non-fractured zones. Besides, the SRV calculation accuracy is lower in comparison with those of the minimum volume ellipsoid algorithm and the Delaunay triangulation

algorithm. When the distribution of microseismic event points is complicated or presents a relatively regular distribution, the cubic method can obtain acceptable model results, but the distribution of microseismic event points is still irregular. Although this single cube method is both simple and efficient, it is in essence a very crude arithmetic method and impractical for the accurate estimation of SRV.

Comparison of results

In order to validate the high accuracy and rationality of the SRV estimation algorithm proposed in this paper, the SRV results based on the mesh subdivision method are compared with those of the Delaunay triangulation algorithm, minimum volume ellipsoid algorithm, and regular cube algorithm as shown in Table 1 :

Table 1 Comparison of results of different fracturing modification volume algorithms

Mesh subdivision algorithm to calculate SRV/(m^3)	Delaunay Triangulation algorithm to calculate SRV/(m^3)	Regular cube model to calculate SRV/(m^3)	Minimum volume ellipsoid algorithm to calculate SRV /(m^3)
688	843	1575	1025

The data in the table clearly shows the relationship between the different SRV calculated by various methods. What is interesting about the data in the table is that the SRV results based on the mesh subdivision algorithm stands out as the most accurate one, followed by the results calculated by the Delaunay triangulation algorithm and by the minimum volume ellipsoid algorithm in sequence with the regular cube operation denoting the most significant SRV error. To sum up, these results have demonstrated the accuracy of analysis in prior sections. Therefore, the method proposed in this paper for calculating SRV based on mesh subdivision is superior in terms of accuracy degree, which sheds light upon the fracture modification effect evaluation.

CONCLUSION

The present study is designed to investigate the effects of different SRV estimation algorithm and it is found that the traditional single-model methods such as cube and ellipsoid are incapable to handle complex microseismic events and unable to effectively eliminate the volume of non-fracture transition zone, which leads the overestimation of SRV. In order to improve the present SRV estimation algorithm and to increase the accuracy of results, this paper proposes a grid-based SRV estimation algorithm which is applicable in complex microseismic event points calculation. This algorithm is composed of three steps. To begin with, the interference of anomalous points should first be eliminated by applying the DBSCAN density clustering algorithm to remove

the anomalous location points in the microseismic event points. In the following step, the initial convex hull is constructed based on the Delaunay triangulation algorithm.

In the third place, the fracture zone is delineated cautiously with the mesh subdivision method so as to improve the model accuracy. Testing result reveals that the mesh subdivision-based SRV estimation algorithm proposed in this paper can eliminate the detrimental effect of non-fracture zones without changing the distribution of original microseismic event points. Furthermore, it can overcome the shortcomings of rough model and the inconspicuous boundary contour lines constructed by traditional methods, which is enlightening for shale fracturing construction design and shale fracturing capacity effect evaluation.

DECLARATIONS

Consent for publication All the authors give consent for the publication.

Conflicts of interest The authors declare no conflicts of interest.

REFERENCES

Alzaalan M E, Aldahdooh R T, Ashour W M (2012) EOPTICS “Enhancement Ordering Points to Identify the Clustering Structure”. International Journal of Computer Applications 40:1-6

Biermann H, Levin A, Zorin D (2000) Piecewise smooth subdivision surfaces with normal control[C]//Proceedings of the 27th annual conference on Computer graphics and interactive techniques:113-120

Chen Y, Tang S, Bouguila N et al (2018) A fast clustering algorithm based on pruning unnecessary distance computations in DBSCAN for high-dimensional data[J]. Pattern Recognition 83:375-387 Cipolla C L, Warpinski N R, Mayerhofer M J, Lolon E P , Vincent M C (2010) The Relationship Between Fracture Complexity, Reservoir Properties, and Fracture-Treatment Design. Spe Production & Operations 25:438-452

Devillers O, Teillaud M (2011) Perturbations for Delaunay and weighted Delaunay 3D triangulations. Comput. Geom 44:160-168

Fisher M K, Heinze J R, Harris C D et al (2004) Optimizing horizontal completion techniques in the Barnett shale using microseismic fracture mapping[C]// SPE Annual Technical Conference and Exhibition. OnePetro

Fisher M, Heinze J, Harris C D, Davidson B, Wright C, Dunn K P (2005) Optimizing horizontal completions in the Barnett shale with microseismic fracture mapping. Journal of Petroleum Technology 57:41-42

Frey P J, Borouchaki H, George P (1998) 3D Delaunay mesh generation coupled with an advancing-front approach. Computer Methods in Applied Mechanics and Engineering 157:115-131

Halder A (2018) On the parameterized computation of minimum volume outer ellipsoid of Minkowski sum of ellipsoids[C]//2018 IEEE Conference on Decision and Control (CDC). IEEE:4040-4045

Hu D, Matzar L, Martysevich V (2014) Effect of natural fractures on eagle ford shale mechanical properties[C]//SPE Annual Technical Conference and Exhibition. OnePetro

Hu K, Zhang Y J (2016) Centroidal Voronoi tessellation based polycube construction for adaptive all- hexahedral mesh generation. Computer Methods in Applied Mechanics and Engineering 305:405- 421

Junhui J I A, Ming H, Xianglei L I U (2018) Surface reconstruction algorithm based on 3d delaunay triangulation[J]. Acta Geodaetica et Cartographica Sinica 47(2):281

Kim J, Cho J (2019) Delaunay triangulation-based spatial clustering technique for enhanced adjacent boundary detection and segmentation of LiDAR 3D point clouds[J]. Sensors 19(18):3926

King G E (2010) Thirty years of gas shale fracturing: what have we learned?[C]// SPE annual technical conference and exhibition. OnePetro

Kumar P, Yildirim E A (2008) Computing Minimum-Volume Enclosing Axis-Aligned Ellipsoids. Journal of Optimization Theory and Applications 136:211-228

Li H, Liu J, Yu H (2018) An Automatic Sparse Pruning Endmember Extraction Algorithm with a Combined Minimum Volume and Deviation Constraint. Remote. Sens 10:509

Mayerhofer M J□Lolon E□Warpinski N R et al (2010) Whatis stimulated reservoir volume?. SPE Production &Operations 25(1):89-98.

Miao W, Liu Y, Shi X et al (2019) A 3D Surface Reconstruction Method Based on Delaunay Triangulation[C]//International Conference on Image and Graphics. Springer, Cham:40-51

Peng S, Ren B, Meng M (2019) Quantifying the influence of fractures for more-accurate laboratory measurement of shale matrix permeability using a modified gas-expansion method[J]. SPE Reservoir Evaluation & Engineering 22(04):1293-1304

Pilevar A H, Sukumar M (2005) GCHL: A mesh-clustering algorithm for high-dimensional very large spatial data bases. Pattern Recognit. Lett 26:999-1010

Ren L, Ran L, Zhao J, Rasouli V, Zhao J, Yang H (2018) Stimulated reservoir volume estimation for shale gas fracturing: Mechanism and modeling approach. Journal of Petroleum Science and Engineering 166:290-304

Roy S, Bhattacharyya D K (2005) An approach to find embedded clusters using density based techniques[C]//International Conference on Distributed Computing and Internet Technology. Springer, Berlin, Heidelberg:523-535

Sakhaee P A, Bryant S L (2012) Gas Permeability of Shale. Spe Reservoir Evaluation & Engineering 15:401-409

Seale R A, Donaldson J, Athans J (2006) Multistage fracturing system: Improving operational efficiency and production[C]//SPE Eastern Regional Meeting. OnePetro

Shao Y Y, Huang X R, Xing Y (2018) Comparative study of SRV fitting methods based on microseismic event points[J]. Journal of Southwest Petroleum University (Natural Science Edition) 40(04):132- 142

Shao Y, Huang X, Xing Y (2017)An integrated study on the sensitivity and uncertainty associated with the evaluation of stimulated reservoir volume (SRV). Journal of Petroleum Science and Engineering 159:903-914

Sheridan K, Puranik T G, Mangortey E et al (2020) An application of dbscan clustering for flight anomaly detection during the approach phase[C]// AIAA Scitech 2020 Forum:1851

Tao J, Zhang W, Lu C (2017) Global linear convergent algorithm to compute the minimum volume enclosing ellipsoid[J]. arXiv preprint arXiv:1702.06254

Todd M J, Yıldırım E A (2007) On Khachiyan's algorithm for the computation of minimum-volume enclosing ellipsoids[J]. Discrete Applied Mathematics 155(13):1731-1744

Walton I, McLennan J (2013) The role of natural fractures in shale gas production[C]//ISRM international conference for effective and sustainable hydraulic fracturing. OnePetro

Wang X L, Li Y H, Wang P et al (2021) Estimation and application of SRV for microseismic data based on improved the Delaunay triangulation algorithm[J]. Advances in Geophysics 36(02):689-695 Warpinski N R, Mayerhofer M J, Vincent M C et al (2009) Stimulating unconventional reservoirs: maximizing network growth while optimizing fracture conductivity[J]. Journal of Canadian Petroleum Technology 48(10): 39-51

Mao D, Miller D S, Karanikas J M et al (2017) Influence of finite hydraulic-fracture conductivity on unconventional hydrocarbon recovery with horizontal wells[J]. SPE Journal 22(06):1790-1807

Wen Q Z, Gao J J, Li Y et al (2014) Analysis of factors influencing SRV in shale reservoirs[J]. Journal of Xi'an University of Petroleum (Natural Science Edition) 29(06):58-64+9

Weng X, Kresse O, Cohen C, Wu R, Gu H (2011) Modeling of Hydraulic Fracture Network Propagation in a Naturally Fractured Formation. Spe Production & Operations 26:368-380

Xie J, Yang C, Gupta N et al Integration of shale- gas-production data and microseismic for fracture andreservoir properties with the fast marching method L.SPE Journal 2015,20(2):347-359

Xu S, Wang C, Zhuang L et al (2019) DBSCAN Clustering Algorithm for the Detection of Nearby Open Clusters Based on Gaia-DR2two[J]. Chinese Astronomy and Astrophysics 43(2): 225-236

Xu W, Le Calvez J H, Thiercelin M J (2009) Characterization of hydraulically-induced fracture network using treatment and microseismic data in a tight-gas sand formation: a geomechanical approach[C]//SPE tight gas completions conference. OnePetro

Yu G Aguilera R (2012) 3D analytical modeling of hydraulicfracturing stimulated reservoir volume [A]//SPE LatinAmerica and Caribbean Petroleum EngineeringConference. Society of Petroleum Engineers[C]:1-16

Zhou H, Jin M, Wu H (2013) A distributed delaunay triangulation algorithm based on centroidal voronoi tessellation for wireless sensor networks[C]// Proceedings of the fourteenth ACM international symposium on Mobile ad hoc networking and computing:59-68